

Measurement of b Hadron Lifetimes in Exclusive Decays Containing a J/ψ in $p\bar{p}$ Collisions at $\sqrt{s} = 1.96$ TeV

- T. Aaltonen,²² B. Álvarez González,^{10,w} S. Amerio,^{42a} D. Amidei,³³ A. Anastassov,³⁷ A. Annovi,¹⁸ J. Antos,¹³ G. Apollinari,¹⁶ J. A. Appel,¹⁶ A. Apresyan,⁴⁷ T. Arisawa,⁵⁶ A. Artikov,¹⁴ J. Asaadi,⁵² W. Ashmanskas,¹⁶ B. Auerbach,⁵⁹ A. Aurisano,⁵² F. Azfar,⁴¹ W. Badgett,¹⁶ A. Barbaro-Galtieri,²⁷ V. E. Barnes,⁴⁷ B. A. Barnett,²⁴ P. Barria,^{45c,45a} P. Bartos,¹³ M. Baucé,^{42b,42a} G. Bauer,³¹ F. Bedeschi,^{45a} D. Beecher,²⁹ S. Behari,²⁴ G. Bellettini,^{45b,45a} J. Bellinger,⁵⁸ D. Benjamin,¹⁵ A. Beretvas,¹⁶ A. Bhatti,⁴⁹ M. Binkley,^{16,a} D. Bisello,^{42b,42a} I. Bizjak,^{29,dd} K. R. Bland,⁵ C. Blocker,⁷ B. Blumenfeld,²⁴ A. Bocci,¹⁵ A. Bodek,⁴⁸ D. Bortoletto,⁴⁷ J. Boudreau,⁴⁶ A. Boveia,¹² B. Brau,^{16,b} L. Brigliadori,^{6b,6a} A. Brisuda,¹³ C. Bromberg,³⁴ E. Brucken,²² M. Bucciantonio,^{45b,45a} J. Budagov,¹⁴ H. S. Budd,⁴⁸ S. Budd,²³ K. Burkett,¹⁶ G. Busetto,^{42b,42a} P. Bussey,²⁰ A. Buzatu,³² S. Cabrera,^{15,y} C. Calancha,³⁰ S. Camarda,⁴ M. Campanelli,³⁴ M. Campbell,³³ F. Canelli,^{12,16} A. Canepa,⁴⁴ B. Carls,²³ D. Carlsmith,⁵⁸ R. Carosi,^{45a} S. Carrillo,^{17,l} S. Carron,¹⁶ B. Casal,¹⁰ M. Casarsa,¹⁶ A. Castro,^{6b,6a} P. Catastini,¹⁶ D. Cauz,^{53a} V. Cavaliere,^{45c,45a} M. Cavalli-Sforza,⁴ A. Cerri,^{27,g} L. Cerrito,^{29,r} Y. C. Chen,¹ M. Chertok,⁸ G. Chiarelli,^{45a} G. Chlachidze,¹⁶ F. Chlebana,¹⁶ K. Cho,²⁶ D. Chokheli,¹⁴ J. P. Chou,²¹ W. H. Chung,⁵⁸ Y. S. Chung,⁴⁸ C. I. Ciobanu,⁴³ M. A. Ciocci,^{45c,45a} A. Clark,¹⁹ D. Clark,⁷ G. Compostella,^{42b,42a} M. E. Convery,¹⁶ J. Conway,⁸ M. Corbo,⁴³ M. Cordelli,¹⁸ C. A. Cox,⁸ D. J. Cox,⁸ F. Crescioli,^{45b,45a} C. Cuenca Almenar,⁵⁹ J. Cuevas,^{10,w} R. Culbertson,¹⁶ D. Dagenhart,¹⁶ N. d'Ascenzo,^{43,u} M. Datta,¹⁶ P. de Barbaro,⁴⁸ S. De Cecco,^{50a} G. De Lorenzo,⁴ M. Dell'Orso,^{45b,45a} C. Deluca,⁴ L. Demortier,⁴⁹ J. Deng,^{15,d} M. Deninno,^{6a} F. Devoto,²² M. d'Errico,^{42b,42a} A. Di Canto,^{45b,45a} B. Di Ruzza,^{45a} J. R. Dittmann,⁵ M. D'Onofrio,²⁸ S. Donati,^{45b,45a} P. Dong,¹⁶ T. Dorigo,^{42a} K. Ebina,⁵⁶ A. Elagin,⁵² A. Eppig,³³ R. Erbacher,⁸ D. Errede,²³ S. Errede,²³ N. Ershaidat,^{43,bb} R. Eusebi,⁵² H. C. Fang,²⁷ S. Farrington,⁴¹ M. Feindt,²⁵ J. P. Fernandez,³⁰ C. Ferrazza,^{45d,45a} R. Field,¹⁷ G. Flanagan,^{47,s} R. Forrest,⁸ M. J. Frank,⁵ M. Franklin,²¹ J. C. Freeman,¹⁶ I. Furic,¹⁷ M. Gallinaro,⁴⁹ J. Galyardt,¹¹ J. E. Garcia,¹⁹ A. F. Garfinkel,⁴⁷ P. Garosi,^{45c,45a} H. Gerberich,²³ E. Gerchtein,¹⁶ S. Giagu,^{50b,50a} V. Giakoumopoulou,³ P. Giannetti,^{45a} K. Gibson,⁴⁶ C. M. Ginsburg,¹⁶ N. Giokaris,³ P. Giromini,¹⁸ M. Giunta,^{45a} G. Giurgiu,²⁴ V. Glagolev,¹⁴ D. Glenzinski,¹⁶ M. Gold,³⁶ D. Goldin,⁵² N. Goldschmidt,¹⁷ A. Golosanov,¹⁶ G. Gomez,¹⁰ G. Gomez-Ceballos,³¹ M. Goncharov,³¹ O. González,³⁰ I. Gorelov,³⁶ A. T. Goshaw,¹⁵ K. Goulianos,⁴⁹ A. Gresele,^{42a} S. Grinstein,⁴ C. Grossi-Pilcher,¹² R. C. Group,¹⁶ J. Guimaraes da Costa,²¹ Z. Gunay-Unalan,³⁴ C. Haber,²⁷ S. R. Hahn,¹⁶ E. Halkiadakis,⁵¹ A. Hamaguchi,⁴⁰ J. Y. Han,⁴⁸ F. Happacher,¹⁸ K. Hara,⁵⁴ D. Hare,⁵¹ M. Hare,⁵⁵ R. F. Harr,⁵⁷ K. Hatakeyama,⁵ C. Hays,⁴¹ M. Heck,²⁵ J. Heinrich,⁴⁴ M. Herndon,⁵⁸ S. Hewamanage,⁵ D. Hidas,⁵¹ A. Hocker,¹⁶ W. Hopkins,^{16,h} D. Horn,²⁵ S. Hou,¹ R. E. Hughes,³⁸ M. Hurwitz,¹² U. Husemann,⁵⁹ N. Hussain,³² M. Hussein,³⁴ J. Huston,³⁴ G. Introzzi,^{45a} M. Iori,^{50b,50a} A. Ivanov,^{8,p} E. James,¹⁶ D. Jang,¹¹ B. Jayatilaka,¹⁵ E. J. Jeon,²⁶ M. K. Jha,^{6a} S. Jindariani,¹⁶ W. Johnson,⁸ M. Jones,⁴⁷ K. K. Joo,²⁶ S. Y. Jun,¹¹ T. R. Junk,¹⁶ T. Kamon,⁵² P. E. Karchin,⁵⁷ Y. Kato,^{40,o} W. Ketchum,¹² J. Keung,⁴⁴ V. Khotilovich,⁵² B. Kilminster,¹⁶ D. H. Kim,²⁶ H. S. Kim,²⁶ H. W. Kim,²⁶ J. E. Kim,²⁶ M. J. Kim,¹⁸ S. B. Kim,²⁶ S. H. Kim,⁵⁴ Y. K. Kim,¹² N. Kimura,⁵⁶ S. Klimentko,¹⁷ K. Kondo,⁵⁶ D. J. Kong,²⁶ J. Konigsberg,¹⁷ A. Korytov,¹⁷ A. V. Kotwal,¹⁵ M. Kreps,²⁵ J. Kroll,⁴⁴ D. Krop,¹² N. Krumnack,^{5,m} M. Kruse,¹⁵ V. Krutelyov,^{52,e} T. Kuhr,²⁵ M. Kurata,⁵⁴ S. Kwang,¹² A. T. Laasanen,⁴⁷ L. Labarga,^{30,cc} S. Lami,^{45a} S. Lammel,¹⁶ M. Lancaster,²⁹ R. L. Lander,⁸ K. Lannon,^{38,v} A. Lath,⁵¹ G. Latino,^{45c,45a} I. Lazzizzera,^{42a} T. LeCompte,² E. Lee,⁵² H. S. Lee,¹² J. S. Lee,²⁶ S. W. Lee,^{52,x} S. Leo,^{45b,45a} S. Leone,^{45a} J. D. Lewis,¹⁶ C.-J. Lin,²⁷ J. Linacre,⁴¹ M. Lindgren,¹⁶ E. Lipeles,⁴⁴ A. Lister,¹⁹ D. O. Litvintsev,¹⁶ C. Liu,⁴⁶ Q. Liu,⁴⁷ T. Liu,¹⁶ S. Lockwitz,⁵⁹ N. S. Lockyer,⁴⁴ A. Loginov,⁵⁹ D. Lucchesi,^{42b,42a} J. Lueck,²⁵ P. Lukens,¹⁶ G. Lungu,⁴⁹ J. Lys,²⁷ R. Lysak,¹³ R. Madrak,¹⁶ K. Maeshima,¹⁶ K. Makhoul,³¹ P. Maksimovic,²⁴ S. Malde,⁴¹ S. Malik,⁴⁹ G. Manca,^{28,c} A. Manousakis-Katsikakis,³ F. Margaroli,⁴⁷ C. Marino,²⁵ M. Martínez,⁴ R. Martínez-Ballarín,³⁰ P. Mastrandrea,^{50a} M. Mathis,²⁴ M. E. Mattson,⁵⁷ P. Mazzanti,^{6a} K. S. McFarland,⁴⁸ P. McIntyre,⁵² R. McNulty,^{28,j} A. Mehta,²⁸ P. Mehtala,²² A. Menzione,^{45a} C. Mesropian,⁴⁹ T. Miao,¹⁶ D. Mietlicki,³³ A. Mitra,¹ H. Miyake,⁵⁴ S. Moed,²¹ N. Moggi,^{6a} M. N. Mondragon,^{16,l} C. S. Moon,²⁶ R. Moore,¹⁶ M. J. Morello,¹⁶ J. Morlock,²⁵ P. Movilla Fernandez,¹⁶ A. Mukherjee,¹⁶ Th. Muller,²⁵ P. Murat,¹⁶ M. Mussini,^{6b,6a} J. Nachtman,^{16,n} Y. Nagai,⁵⁴ J. Naganoma,⁵⁶ I. Nakano,³⁹ A. Napier,⁵⁵ J. Nett,⁵⁸ C. Neu,^{44,aa} M. S. Neubauer,²³ J. Nielsen,^{27,f} L. Nodulman,² O. Norniella,²³ E. Nurse,²⁹ L. Oakes,⁴¹ S. H. Oh,¹⁵ Y. D. Oh,²⁶ I. Oksuzian,¹⁷ T. Okusawa,⁴⁰ R. Orava,²² L. Ortolan,⁴ S. Pagan Griso,^{42b,42a} C. Pagliarone,^{53a} E. Palencia,^{10,g} V. Papadimitriou,¹⁶ A. A. Paramonov,² J. Patrick,¹⁶ G. Pauletta,^{53b,53a} M. Paulini,¹¹ C. Paus,³¹ D. E. Pellett,⁸ A. Penzo,^{53a} T. J. Phillips,¹⁵ G. Piacentino,^{45a} E. Pianori,⁴⁴ J. Pilot,³⁸ K. Pitts,²³ C. Plager,⁹ L. Pondrom,⁵⁸ K. Potamianos,⁴⁷ O. Poukhov,^{14,a} F. Prokoshin,^{14,z} A. Pronko,¹⁶ F. Ptoshos,^{18,i} E. Pueschel,¹¹ G. Punzi,^{45b,45a} J. Pursley,⁵⁸ A. Rahaman,⁴⁶ V. Ramakrishnan,⁵⁸ N. Ranjan,⁴⁷

- I. Redondo,³⁰ P. Renton,⁴¹ M. Rescigno,^{50a} F. Rimondi,^{6b,6a} L. Ristori,^{45a,16} A. Robson,²⁰ T. Rodrigo,¹⁰ T. Rodriguez,⁴⁴ E. Rogers,²³ S. Rolli,⁵⁵ R. Roser,¹⁶ M. Rossi,^{53a} F. Ruffini,^{45c,45a} A. Ruiz,¹⁰ J. Russ,¹¹ V. Rusu,¹⁶ A. Safonov,⁵² W. K. Sakamoto,⁴⁸ L. Santi,^{53b,53a} L. Sartori,^{45a} K. Sato,⁵⁴ V. Saveliev,^{43,u} A. Savoy-Navarro,⁴³ P. Schlabach,¹⁶ A. Schmidt,²⁵ E. E. Schmidt,¹⁶ M. P. Schmidt,^{59,a} M. Schmitt,³⁷ T. Schwarz,⁸ L. Scodellaro,¹⁰ A. Scribano,^{45c,45a} F. Scuri,^{45a} A. Sedov,⁴⁷ S. Seidel,³⁶ Y. Seiya,⁴⁰ A. Semenov,¹⁴ F. Sforza,^{45b,45a} A. Sfyrla,²³ S. Z. Shalhout,⁸ T. Shears,²⁸ P. F. Shepard,⁴⁶ M. Shimojima,^{54,t} S. Shiraishi,¹² M. Shochet,¹² I. Shreyber,³⁵ A. Simonenko,¹⁴ P. Sinervo,³² A. Sissakian,^{14,a} K. Sliwa,⁵⁵ J. R. Smith,⁸ F. D. Snider,¹⁶ A. Soha,¹⁶ S. Somalwar,⁵¹ V. Sorin,⁴ P. Squillaciotti,¹⁶ M. Stanitzki,⁵⁹ R. St. Denis,²⁰ B. Stelzer,³² O. Stelzer-Chilton,³² D. Stentz,³⁷ J. Strologas,³⁶ G. L. Strycker,³³ Y. Sudo,⁵⁴ A. Sukhanov,¹⁷ I. Suslov,¹⁴ K. Takemasa,⁵⁴ Y. Takeuchi,⁵⁴ J. Tang,¹² M. Tecchio,³³ P. K. Teng,¹ J. Thom,^{16,h} J. Thome,¹¹ G. A. Thompson,²³ E. Thomson,⁴⁴ P. Ttito-Guzmán,³⁰ S. Tkaczyk,¹⁶ D. Toback,⁵² S. Tokar,¹³ K. Tollefson,³⁴ T. Tomura,⁵⁴ D. Tonelli,¹⁶ S. Torre,¹⁸ D. Torretta,¹⁶ P. Totaro,^{53b,53a} M. Trovato,^{45d,45a} Y. Tu,⁴⁴ N. Turini,^{45c,45a} F. Ukegawa,⁵⁴ S. Uozumi,²⁶ A. Varganov,³³ E. Vataga,^{45d,45a} F. Vázquez,^{17,l} G. Velev,¹⁶ C. Vellidis,³ M. Vidal,³⁰ I. Vila,¹⁰ R. Vilar,³² M. Vogel,³⁶ G. Volpi,^{45b,45a} P. Wagner,⁴⁴ R. L. Wagner,¹⁶ T. Wakisaka,⁴⁰ R. Wallny,⁹ S. M. Wang,¹ A. Warburton,³² D. Waters,²⁹ M. Weinberger,⁵² H. Wenzel,¹⁶ W. C. Wester III,¹⁶ B. Whitehouse,⁵⁵ D. Whiteson,^{44,d} A. B. Wicklund,² E. Wicklund,¹⁶ S. Wilbur,¹² F. Wick,²⁵ H. H. Williams,⁴⁴ J. S. Wilson,³⁸ P. Wilson,¹⁶ B. L. Winer,³⁸ P. Wittich,^{16,h} S. Wolbers,¹⁶ H. Wolfe,³⁸ T. Wright,³³ X. Wu,¹⁹ Z. Wu,⁵ K. Yamamoto,⁴⁰ J. Yamaoka,¹⁵ T. Yang,¹⁶ U. K. Yang,^{12,q} Y. C. Yang,²⁶ W.-M. Yao,²⁷ G. P. Yeh,¹⁶ K. Yi,^{16,n} J. Yoh,¹⁶ K. Yorita,⁵⁶ T. Yoshida,^{40,k} G. B. Yu,¹⁵ I. Yu,²⁶ S. S. Yu,¹⁶ J. C. Yun,¹⁶ A. Zanetti,^{53a} Y. Zeng,¹⁵ and S. Zucchelli^{6b,6a}

(CDF Collaboration)

¹*Institute of Physics, Academia Sinica, Taipei, Taiwan 11529, Republic of China*²*Argonne National Laboratory, Argonne, Illinois 60439, USA*³*University of Athens, 157 71 Athens, Greece*⁴*Institut de Fisica d'Altes Energies, Universitat Autònoma de Barcelona, E-08193, Bellaterra (Barcelona), Spain*⁵*Baylor University, Waco, Texas 76798, USA*^{6a}*Istituto Nazionale di Fisica Nucleare Bologna, I-40127 Bologna, Italy*^{6b}*University of Bologna, I-40127 Bologna, Italy*⁷*Brandeis University, Waltham, Massachusetts 02254, USA*⁸*University of California, Davis, Davis, California 95616, USA*⁹*University of California, Los Angeles, Los Angeles, California 90024, USA*¹⁰*Instituto de Fisica de Cantabria, CSIC-University of Cantabria, 39005 Santander, Spain*¹¹*Carnegie Mellon University, Pittsburgh, Pennsylvania 15213, USA*¹²*Enrico Fermi Institute, University of Chicago, Chicago, Illinois 60637, USA*¹³*Comenius University, 842 48 Bratislava, Slovakia; Institute of Experimental Physics, 040 01 Kosice, Slovakia*¹⁴*Joint Institute for Nuclear Research, RU-141980 Dubna, Russia*¹⁵*Duke University, Durham, North Carolina 27708, USA*¹⁶*Fermi National Accelerator Laboratory, Batavia, Illinois 60510, USA*¹⁷*University of Florida, Gainesville, Florida 32611, USA*¹⁸*Laboratori Nazionali di Frascati, Istituto Nazionale di Fisica Nucleare, I-00044 Frascati, Italy*¹⁹*University of Geneva, CH-1211 Geneva 4, Switzerland*²⁰*Glasgow University, Glasgow G12 8QQ, United Kingdom*²¹*Harvard University, Cambridge, Massachusetts 02138, USA*²²*Division of High Energy Physics, Department of Physics, University of Helsinki and Helsinki Institute of Physics, FIN-00014, Helsinki, Finland*²³*University of Illinois, Urbana, Illinois 61801, USA*²⁴*The Johns Hopkins University, Baltimore, Maryland 21218, USA*²⁵*Institut für Experimentelle Kernphysik, Karlsruhe Institute of Technology, D-76131 Karlsruhe, Germany*²⁶*Center for High Energy Physics: Kyungpook National University, Daegu 702-701, Korea; Seoul National University, Seoul 151-742, Korea; Sungkyunkwan University, Suwon 440-746, Korea; Korea Institute of Science and Technology Information, Daejeon 305-806, Korea; Chonnam National University, Gwangju 500-757, Korea; Chonbuk National University, Jeonju 561-756, Korea*²⁷*Ernest Orlando Lawrence Berkeley National Laboratory, Berkeley, California 94720, USA*²⁸*University of Liverpool, Liverpool L69 7ZE, United Kingdom*²⁹*University College London, London WC1E 6BT, United Kingdom*³⁰*Centro de Investigaciones Energeticas Medioambientales y Tecnologicas, E-28040 Madrid, Spain*³¹*Massachusetts Institute of Technology, Cambridge, Massachusetts 02139, USA*

- ³²Institute of Particle Physics: McGill University, Montréal, Québec, Canada H3A 2T8; Simon Fraser University, Burnaby, British Columbia, Canada V5A 1S6; University of Toronto, Toronto, Ontario, Canada M5S 1A7;
 and TRIUMF, Vancouver, British Columbia, Canada V6T 2A3
- ³³University of Michigan, Ann Arbor, Michigan 48109, USA
- ³⁴Michigan State University, East Lansing, Michigan 48824, USA
- ³⁵Institution for Theoretical and Experimental Physics, ITEP, Moscow 117259, Russia
- ³⁶University of New Mexico, Albuquerque, New Mexico 87131, USA
- ³⁷Northwestern University, Evanston, Illinois 60208, USA
- ³⁸The Ohio State University, Columbus, Ohio 43210, USA
- ³⁹Okayama University, Okayama 700-8530, Japan
- ⁴⁰Osaka City University, Osaka 588, Japan
- ⁴¹University of Oxford, Oxford OX1 3RH, United Kingdom
- ^{42a}Istituto Nazionale di Fisica Nucleare, Sezione di Padova-Trento, I-35131 Padova, Italy
- ^{42b}University of Padova, I-35131 Padova, Italy
- ⁴³LPNHE, Université Pierre et Marie Curie/IN2P3-CNRS, UMR7585, Paris, F-75252 France
- ⁴⁴University of Pennsylvania, Philadelphia, Pennsylvania 19104, USA
- ^{45a}Istituto Nazionale di Fisica Nucleare Pisa, I-56127 Pisa, Italy
- ^{45b}University of Pisa, I-56127 Pisa, Italy
- ^{45c}University of Siena, I-56127 Pisa, Italy
- ^{45d}Scuola Normale Superiore, I-56127 Pisa, Italy
- ⁴⁶University of Pittsburgh, Pittsburgh, Pennsylvania 15260, USA
- ⁴⁷Purdue University, West Lafayette, Indiana 47907, USA
- ⁴⁸University of Rochester, Rochester, New York 14627, USA
- ⁴⁹The Rockefeller University, New York, New York 10065, USA
- ^{50a}Istituto Nazionale di Fisica Nucleare, Sezione di Roma I
- ^{50b}Sapienza Università di Roma, I-00185 Roma, Italy
- ⁵¹Rutgers University, Piscataway, New Jersey 08855, USA
- ⁵²Texas A&M University, College Station, Texas 77843, USA
- ^{53a}Istituto Nazionale di Fisica Nucleare Trieste/Udine, I-34100 Trieste
- ^{53b}University of Trieste/Udine, I-34100 Udine, Italy
- ⁵⁴University of Tsukuba, Tsukuba, Ibaraki 305, Japan
- ⁵⁵Tufts University, Medford, Massachusetts 02155, USA
- ⁵⁶Waseda University, Tokyo 169, Japan
- ⁵⁷Wayne State University, Detroit, Michigan 48201, USA
- ⁵⁸University of Wisconsin, Madison, Wisconsin 53706, USA
- ⁵⁹Yale University, New Haven, Connecticut 06520, USA

(Received 15 December 2010; published 24 March 2011)

We report on a measurement of b -hadron lifetimes in the fully reconstructed decay modes $B^+ \rightarrow J/\psi K^+$, $B^0 \rightarrow J/\psi K^*(892)^0$, $B^0 \rightarrow J/\psi K_s^0$, and $\Lambda_b^0 \rightarrow J/\psi \Lambda^0$ using data corresponding to an integrated luminosity of 4.3 fb^{-1} , collected by the CDF II detector at the Fermilab Tevatron. The measured lifetimes are $\tau(B^+) = [1.639 \pm 0.009(\text{stat}) \pm 0.009(\text{syst})] \text{ ps}$, $\tau(B^0) = [1.507 \pm 0.010(\text{stat}) \pm 0.008(\text{syst})] \text{ ps}$, and $\tau(\Lambda_b^0) = [1.537 \pm 0.045(\text{stat}) \pm 0.014(\text{syst})] \text{ ps}$. The lifetime ratios are $\tau(B^+)/\tau(B^0) = [1.088 \pm 0.009(\text{stat}) \pm 0.004(\text{syst})]$ and $\tau(\Lambda_b^0)/\tau(B^0) = [1.020 \pm 0.030(\text{stat}) \pm 0.008(\text{syst})]$. These are the most precise determinations of these quantities from a single experiment.

DOI: 10.1103/PhysRevLett.106.121804

PACS numbers: 13.25.Hw, 13.30.Eg, 14.20.Mr, 14.40.Nd

The lifetime of ground-state hadrons containing a b quark and lighter quarks is largely determined by the charged weak decay of the b quark. Interactions involving the lighter quarks, referred to as spectator processes, alter b -hadron lifetimes at approximately the 10% level. Lifetimes are important to probe our understanding of the low-energy strong interaction. While precise predictions for b -hadron lifetimes are difficult to calculate, ratios are predicted with fairly high accuracy by the heavy quark expansion (HQE) [1]. This framework of theoretical calculation is used to predict low-energy QCD effects in many

flavor observables. For example, HQE predicts the decay width of B_s mesons to final states common to B_s^0 and \bar{B}_s^0 , Γ_{12}^s , which enters the decay-width difference in the B_s^0 system and several CP violation effects. The measurement of lifetime ratios provides a simple and accurate way to test the HQE framework as nonstandard model effects are expected to be highly suppressed in lifetimes. The ratio $\tau(B^+)/\tau(B^0)$, R_+ (charge conjugates are implied throughout) is predicted to be in the range 1.04–1.08 [1–4]. Predictions for the ratio $\tau(\Lambda_b^0)/\tau(B^0)$, R_Λ in HQE, which do not presently incorporate next-to-leading order QCD

corrections, lie in the range 0.88 ± 0.05 [2,4,5]. The first measurements of the Λ_b^0 lifetime have been at the lower end of that range. However, recent high precision measurements by the CDF experiment [6,7] based on 1.0 fb^{-1} of data, are significantly higher than previous results. It is therefore useful to keep pursuing lifetime measurements with increased precision to settle the issue. In this Letter we report precise measurements of b -quark meson lifetimes using the channels $B^+ \rightarrow J/\psi K^+$, $B^0 \rightarrow J/\psi K^{*0}$, and $B^0 \rightarrow J/\psi K_s^0$, in addition to the lifetime of the Λ_b^0 baryon using the $\Lambda_b^0 \rightarrow J/\psi \Lambda^0$ decay channel. Our data sample corresponds to an integrated luminosity of 4.3 fb^{-1} and consists of $p\bar{p}$ collisions at a center of mass energy $\sqrt{s} = 1.96 \text{ TeV}$ collected by the CDF II detector at the Fermilab Tevatron. The measurement reported here improves the previous CDF measurement [6] of the Λ_b^0 lifetime by updating it with significantly more data. In all decay modes, the decay position of the b hadron is estimated using only J/ψ decay products so that differences in decay time resolution between channels is reduced and certain systematic uncertainties cancel in ratios of lifetimes.

The components of the CDF II detector relevant to this analysis are described briefly here. Charged particles are reconstructed using six layers of silicon microstrip detectors with radii between 2.4 and 23 cm [8] and an open-cell drift chamber called the central outer tracker (COT) [9]. These are immersed in a 1.4 T solenoidal magnetic field and cover the range $|\eta| \leq 1$, where η is the pseudorapidity defined as $\eta \equiv -\ln \tan(\theta/2)$, and θ is the polar angle [10]. Four layers of planar drift chambers (CMU) [11] detect muons with $p_T > 1.4 \text{ GeV}/c$ within $|\eta| < 0.6$. Additional chambers and scintillators (CMX) [12] cover $0.6 < |\eta| < 1.0$ for muons with $p_T > 2.0 \text{ GeV}/c$.

The reconstruction of b -hadron candidates begins with the collection of $J/\psi \rightarrow \mu^+ \mu^-$ candidates using a dimuon trigger. The extremely fast tracker (XFT) [13] uses COT hit information to measure the transverse momentum and azimuthal direction of charged tracks. Events with $J/\psi \rightarrow \mu^+ \mu^-$ candidates are recorded for further analysis if two or more extrapolated tracks are matched to CMU or CMX track segments, opposite-charge and opening-angle requirements are met, and the J/ψ candidate has mass in the range 2.7 to $4.0 \text{ GeV}/c^2$. After offline reconstruction, tracks corresponding to two triggered muon candidates are constrained to originate from a common vertex to make a $J/\psi \rightarrow \mu^+ \mu^-$ candidate. To ensure a high-quality vertex for the lifetime measurement, each muon track is required to have at least three hits in the silicon system. The reconstructed $\mu^+ \mu^-$ invariant mass is required to be in the range $3.014 < m(\mu\mu) < 3.174 \text{ GeV}/c^2$. The b hadron is assumed to originate from the average beam spot determined as a function of time using inclusive jet data. The primary vertex for a given event is the x - y position of this beam spot at the average z coordinate of the muon tracks at their closest approach to the beam line. The typical beam

line size is $\approx 30 \mu\text{m}$ in x - y , and this dominates the uncertainty on the decay length. The projection of the transverse decay vector onto the b -hadron p_T direction L_{xy} and its uncertainty σ_{xy} are also obtained and are used to estimate the proper decay time $ct = \frac{ML_{xy}}{p_T}$ and its uncertainty σ^{ct} , where M and p_T are the mass and transverse momentum of the b hadron. The uncertainties in the primary and J/ψ vertices, and the transverse momentum are all included in σ^{ct} which has a typical value around 0.1 ps. Uncertainties in transverse momentum have a negligible effect on ct measurement, in comparison to the uncertainty on the vertex positions.

We reconstruct $K^{*0} \rightarrow K^+ \pi^-$, $K_s^0 \rightarrow \pi^+ \pi^-$, and $\Lambda^0 \rightarrow p \pi^-$ candidates from pairs of oppositely charged tracks fit to a common vertex. As K_s^0 and Λ^0 decays can occur outside some layers of the silicon system due to their long lifetime, their tracks are not required to have silicon hits. The fitted mass is required to be in a mass window; for the K^{*0} this window is $0.84 < m(K\pi) < 0.96 \text{ GeV}/c^2$ (the lower range is selected in order to avoid reflections from the $\phi \rightarrow K^+ K^-$, where one kaon is misreconstructed as a pion), for the K_s^0 it is $0.473 < m(\pi\pi) < 0.523 \text{ GeV}/c^2$, and for the Λ^0 it is $1.107 < m(p\pi) < 1.125 \text{ GeV}/c^2$. This corresponds to approximately $\pm 3\sigma$, where σ is the mass resolution of the reconstructed signal. We suppress K_s^0 and Λ^0 cross contamination by rejecting K_s^0 (Λ^0) candidates with proton-pion (pion-pion) invariant mass consistent with Λ^0 (K_s^0). We reconstruct the b hadrons by performing a kinematic fit of all b -hadron final state tracks to the appropriate topology: two spatially separated vertices in the case of $\Lambda_b^0 \rightarrow J/\psi \Lambda^0$ and $B^0 \rightarrow J/\psi K_s^0$, one vertex in all other cases. A mass constraint is applied in the J/ψ fit, and the reconstructed momenta of the K_s^0 and Λ^0 are required to point back to the J/ψ vertex. We exclude candidates with $\sigma^{ct} > 100 \mu\text{m}$ to ensure well measured vertices. Additional selection requirements implying consistency with the fit assumptions (common vertex or vertices, mass and pointing constraints) are also applied. Further selection requirements on the transverse momenta of the b hadrons and daughter particles, invariant mass of the K_s^0 , K^{*0} , and Λ^0 , the vertex probability of the b hadrons, and the L_{xy} significance of the K_s^0 and Λ^0 were obtained via an optimization procedure, which maximizes the quantity $S/\sqrt{S+B}$ over all of the selection requirements. The number of signal events (S) is estimated from simulation and the number of background events (B) from the mass sidebands in data. Sidebands are events away from the mass peak and form a sample of pure background.

For B^+ and B^0 modes, only candidates with a reconstructed B mass between 5.17 and $5.39 \text{ GeV}/c^2$ are used for the lifetime measurements. For the Λ_b^0 mode, the mass range is set to 5.48 – $5.76 \text{ GeV}/c^2$. These ranges provide a sufficient number of events in the sideband regions to constrain the background shape while avoiding regions

where the mass distribution has complex structure. The invariant mass distributions are shown in Fig. 1, where the sideband regions are indicated. The hadron masses are consistent with world average values. We observe the following yields of signal events: $45\,000 \pm 230$ (B^+), $16\,860 \pm 140$ ($B^0 \rightarrow J/\psi K^{*0}$), $12\,070 \pm 120$ ($B^0 \rightarrow J/\psi K_s^0$), and 1710 ± 50 (Λ_b^0).

The lifetimes are extracted using an unbinned maximum likelihood method. The likelihood function \mathcal{L} is multivariate, and is based on the probability of observing a candidate i with reconstructed mass m_i , decay time ct_i , decay time uncertainty σ_i^{ct} , and mass uncertainty σ_i^m . The PDF is factorized in the following form:

$$\mathcal{L} = \prod_i [f_s P_m^s(m_i | \sigma_i^m) T_t^s(ct_i | \sigma_i^{ct}) S_{\sigma^{ct}}^s(\sigma_i^{ct}) + (1 - f_s) P_m^b(m_i) T_t^b(ct_i | \sigma_i^{ct}) S_{\sigma^{ct}}^b(\sigma_i^{ct})], \quad (1)$$

where P_m , T_{ct} , and $S_{\sigma^{ct}}$ are the normalized probability density functions (PDF) for observables m_i , ct_i , and σ_i^{ct} , the superscripts s or b refer to the PDF for signal or background candidates, respectively, and f_s is the fraction of signal events. The PDF $S_{\sigma^{ct}}$ is substantially different for signal and background events and therefore needs to be taken into account as discussed in Ref. [14]. A PDF term for σ_i^m can be ignored as the distribution of σ_i^m is observed to be similar for both signal and background and hence represents a constant in the log-likelihood.

The signal mass distribution P_m^s is modeled as

$$P_m^s = \sum_i \sum_{k=1}^2 \frac{F_k \exp(-\frac{(m_0 - m_i)^2}{2(u_k \sigma_i^m)^2})}{\sqrt{2\pi} u_k \sigma_i^m}, \quad (2)$$

where $F_1 + F_2 = 1$, m_0 is the mass of the hadron, and u_k are scale factors to account for the misestimation of the mass resolutions. We find that two Gaussians are sufficient to model the data. The background mass distribution P_m^b is modeled as a linear function.

The signal ct distribution T_{ct}^s is modeled by an exponential ($e^{-ct_i/c\tau}/c\tau$) convolved with a detailed detector ct -resolution model \mathcal{R} . The background ct distribution T_{ct}^b has four components: a δ function convolved with \mathcal{R} to account for backgrounds from prompt J/ψ 's originating from the primary vertex, and one increasing and two

decreasing exponentials that account for mismeasured decay vertices and background from other heavy-flavor decays. These exponential components are convolved with a single Gaussian of width σ_i^{ct} multiplied by a scale factor. The relative contribution of each background component is determined by the data. The parameters of the background model are mainly determined from the candidates in the mass sidebands. Studies of inclusive b -hadron decays have shown that after the selection requirements the contamination from other b decays is very low and, furthermore, that the mass distribution of the long-lived background components is flat in the fitted mass range, and hence the mass sidebands can provide a realistic background model for candidates in the signal mass range.

The same resolution model \mathcal{R} is used for signal and prompt background events. The detector resolution is based upon a Gaussian with width $s_j \cdot \sigma_i^{ct}$, where s_j is the scale factor that accounts for the misestimation of the σ_i^{ct} . Motivated by a study of resolution in an inclusive sample of J/ψ events, where prompt J/ψ events dominate, \mathcal{R} is modeled as $\mathcal{R} = \sum_{j=1}^3 f_j / (\sqrt{2\pi} s_j \sigma_i^{ct}) \cdot \exp(-t^2 / 2(s_j \sigma_i^{ct})^2)$, where $f_1 + f_2 + f_3 = 1$. The Gaussians are centered at zero as no evidence of an offset in the data samples is observed. Small differences in \mathcal{R} arise between decay channels due to different χ^2 distributions for the vertex fits of decays with different number of tracks. Therefore the parameters f_j and s_j are obtained separately for each channel from a fit to data in the mass sidebands. This yields an accurate determination of \mathcal{R} since the background events are primarily expected to originate from the interaction vertex.

The functional form of the PDF $S_{\sigma^{ct}}$ is determined empirically using data in the B hadron mass sidebands as indicated on Fig. 1. The parameters of the function, which are different for signal and background are determined from the final fit to data. After the resolution model parameters are determined from the mass-sideband only fit, the likelihood is calculated for each candidate and the product is maximized in each of the four channels to extract the lifetime, signal yield, and the other parameters required to describe the mass, background decay time, and σ^{ct} distributions. Decay time projections of the likelihood function are compared with the data in Fig. 2.

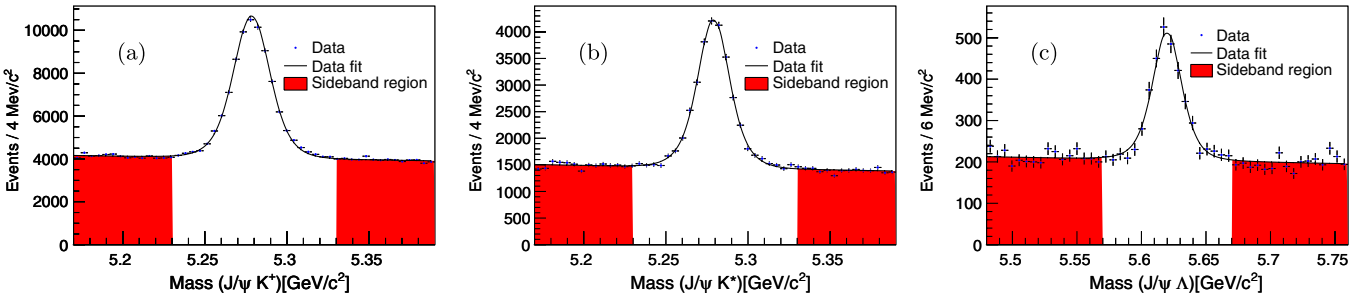
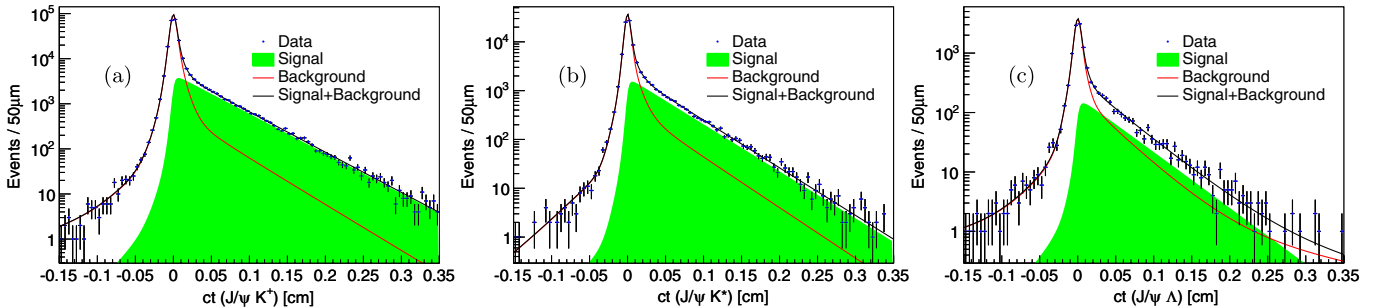


FIG. 1 (color online). Invariant mass together with mass fit projection for (a) $B^+ \rightarrow J/\psi K^+$, (b) $B^0 \rightarrow J/\psi K^*$, and (c) $\Lambda_b^0 \rightarrow J/\psi \Lambda^0$.

FIG. 2 (color online). Decay time distributions for (a) $B^+ \rightarrow J/\psi K^+$, (b) $B^0 \rightarrow J/\psi K^*$, and (c) $\Lambda_b^0 \rightarrow J/\psi \Lambda^0$ candidates.

We considered correlated and uncorrelated systematic uncertainties. Correlated uncertainties affect all measured lifetimes identically, and cancel in ratios. We estimate uncertainties due to any residual misalignments of the silicon detector using Monte Carlo samples generated with radial displacements of individual sensors (internal alignment) and relative translation and rotation of the silicon detector with respect to the COT (global alignment). The XFT triggers on tracks assuming they originate from the center of the beam, which may introduce a bias for triggering long-lived decays. No indication of any bias was found in a study of the XFT response in a large sample of simulated events but a small uncertainty is assigned due to the limited statistical precision of the evaluation method. The systematic uncertainty that results from ignoring the correlation between reconstructed mass and σ^{ct} in the likelihood is found to be negligible. The remainder of systematic uncertainties are treated as uncorrelated. They were determined using pseudoexperiments in which many statistical trials are generated according to alternate PDFs where the alternate parameters are derived from data. The shift in data due to the alternate PDFs were consistent with the shift observed with the pseudoexperiments. As the time resolution is determined from the prompt events, and the shape of those events is sensitive to the modeling of long-lived (positive and negative) background, uncertainties in

the background modeling can affect the lifetime through the resolution function. We account for that uncertainty by including an extra long-lived component in the background model. This alternate description produces a substantial change in the fraction of prompt events (approximately 7%), and has a small but non-negligible effect on the lifetime. A further small uncertainty arising from the functional form of R is also assessed and included in the total resolution uncertainty. To evaluate uncertainties in the mass model, alternate parametrizations, including a second order polynomial for background, and a single Gaussian to describe signal events, were considered. Alternatives to the background PDF included extra long-lived and Gaussian components. We determined the uncertainty due to the σ^{ct} parametrization by using a reasonable alternate model. We also considered the effect of ignoring any differences between signal and background mass uncertainties by using distributions determined from data to generate the values of the mass uncertainty in the pseudoexperiments. We also determined the systematic uncertainty due to the presence of the Cabibbo suppressed channel $B^+ \rightarrow J/\psi \pi^+$ in the charged B decays, and the effect of swapping the kaon and pion hypotheses in K^{*0} reconstruction. The possibility of a systematic biases caused by the σ^{ct} and p_T selection requirements were found to be negligible. The systematic uncertainties are summarized in Table I.

TABLE I. Summary of systematic uncertainties.

	$J/\psi K^+$ (fs)	$J/\psi K^{*0}$ (fs)	$J/\psi K_s^0$ (fs)	$J/\psi \Lambda^0$ (fs)	R_+	R_Λ
Resolution function	2.5	3.5	3.0	8.9	0.0024	0.0061
Background ct model	1.0	2.3	4.1	4.6	0.0017	0.0034
Mass model	2.8	2.8	2.8	2.8	0.0020	0.0017
Proper decay time uncertainty	1.7	1.7	1.7	4.3	0.0010	0.0029
Mass uncertainty	3.0	3.0	3.0	3.0	0.0020	0.0012
Total uncorrelated	± 5.2	± 6.2	± 6.8	± 11.7	0.0042	0.0079
Alignment	6.7	6.7	6.7	6.7
Cabibbo suppressed mode in B^+	0.7	0.0004	...
Swapped track assignment in B^0	...	0.7
Possible trigger bias	1.7	1.7	1.7	1.7
$\sigma^{ct} - m$ correlation	0.7	0.7	0.7	0.7
Total	± 8.7	± 9.3	± 9.7	± 13.7	0.0043	0.0079

We measure $\tau(B^+) = [1.639 \pm 0.009(\text{stat}) \pm 0.009(\text{syst})]$ ps and $\tau(B^0) = [1.507 \pm 0.010(\text{stat}) \pm 0.008(\text{syst})]$ ps where the two B^0 measurements have been combined. These results are consistent and of similar precision to the leading measurements from Belle [15] which are $\tau(B^+) = [1.635 \pm 0.011(\text{stat}) \pm 0.011(\text{syst})]$ ps and $\tau(B^0) = [1.534 \pm 0.008(\text{stat}) \pm 0.010(\text{syst})]$ ps. The similarities between the decay channels allow for the accurate determination of the ratio $R_+ = [1.088 \pm 0.009(\text{stat}) \pm 0.004(\text{syst})]$ which favors a slightly higher value than the current average of 1.071 ± 0.009 [2]. These results are consistent with the current HQE predictions, giving further confidence in this theoretical framework, and also provide an accurate test for future lattice QCD calculations. For the Λ_b^0 we measure $\tau(\Lambda_b^0) = [1.537 \pm (\text{stat})0.045 \pm (\text{syst})0.014]$ ps and $R_\Lambda = [1.020 \pm 0.030(\text{stat}) \pm 0.008(\text{syst})]$. This measurement is the most precise measurement of $\tau(\Lambda_b^0)$ and is consistent with the previous CDF measurement in this decay channel of $\tau(\Lambda_b^0) = [1.593_{-0.078}^{+0.083}(\text{stat}) \pm 0.033(\text{syst})]$ ps [6] but is more than 2σ larger than the world average of $1.383_{-0.048}^{+0.049}$ ps and the previous CDF measurement [7], performed on a different decay channel ($\Lambda_c^\pm \pi^\mp$): $[1.401 \pm 0.046(\text{stat}) \pm 0.035(\text{syst})]$ ps. The ratio is also higher than the predicted values of 0.88 ± 0.95 . In summary, we report the most precise determination of $\tau(B^+)/\tau(B^0)$. It is consistent with other measurements and the predicted value which gives confidence in the HQE framework for flavor observables. We also report the most precise measurement of $\tau(\Lambda_b^0)$, which supports a higher value than the world average and theory predictions.

We thank the Fermilab staff and the technical staffs of the participating institutions for their vital contributions. This work was supported by the U.S. Department of Energy and National Science Foundation; the Italian Istituto Nazionale di Fisica Nucleare; the Ministry of Education, Culture, Sports, Science and Technology of Japan; the Natural Sciences and Engineering Research Council of Canada; the National Science Council of the Republic of China; the Swiss National Science Foundation; the A.P. Sloan Foundation; the Bundesministerium für Bildung und Forschung, Germany; the World Class University Program, the National Research Foundation of Korea; the Science and Technology Facilities Council and the Royal Society, U.K.; the Institut National de Physique Nucléaire et Physique des Particules/CNRS; the Russian Foundation for Basic Research; the Ministerio de Ciencia e Innovación, and Programa Consolider-Ingenio 2010, Spain; the Slovak R&D Agency; and the Academy of Finland.

^aDeceased.

^bVisitor from University of Massachusetts Amherst, Amherst, MA 01003, USA.

^cVisitor from Istituto Nazionale di Fisica Nucleare, Sezione di Cagliari, 09042 Monserrato (Cagliari), Italy.

^dVisitor from University of California Irvine, Irvine, CA 92697, USA.

^eVisitor from University of California Santa Barbara, Santa Barbara, CA 93106, USA.

^fVisitor from University of California Santa Cruz, Santa Cruz, CA 95064, USA.

^gVisitor from CERN, CH-1211 Geneva, Switzerland.

^hVisitor from Cornell University, Ithaca, NY 14853, USA.

ⁱVisitor from University of Cyprus, Nicosia CY-1678, Cyprus.

^jVisitor from University College Dublin, Dublin 4, Ireland.

^kVisitor from University of Fukui, Fukui City, Fukui Prefecture, Japan 910-0017.

^lVisitor from Universidad Iberoamericana, Mexico D.F., Mexico.

^mVisitor from Iowa State University, Ames, IA 50011, USA.

ⁿVisitor from University of Iowa, Iowa City, IA 52242, USA.

^oVisitor from Kinki University, Higashi-Osaka City, Japan 577-8502.

^pVisitor from Kansas State University, Manhattan, KS 66506, USA.

^qVisitor from University of Manchester, Manchester M13 9PL, England.

^rVisitor from Queen Mary, University of London, London, E1 4NS, England.

^sVisitor from Muons, Inc., Batavia, IL 60510, USA.

^tVisitor from Nagasaki Institute of Applied Science, Nagasaki, Japan.

^uVisitor from National Research Nuclear University, Moscow, Russia.

^vVisitor from University of Notre Dame, Notre Dame, IN 46556, USA.

^wVisitor from Universidad de Oviedo, E-33007 Oviedo, Spain.

^xVisitor from Texas Tech University, Lubbock, TX 79609, USA.

^yVisitor from IFIC(CSIC-Universitat de Valencia), 56071 Valencia, Spain.

^zVisitor from Universidad Técnica Federico Santa María, 110v Valparaíso, Chile.

^{aa}Visitor from University of Virginia, Charlottesville, VA 22906, USA.

^{bb}Visitor from Yarmouk University, Irbid 211-63, Jordan.

^{cc}Visitor from Universidad Autónoma de Madrid, Cantoblanco, 28049, Madrid.

^{dd}On leave from J. Stefan Institute, Ljubljana, Slovenia.

- [1] M. Beneke *et al.*, *Nucl. Phys.* **B639**, 389 (2002); E. Franco, V. Lubicz, F. Mescia, and C. Tarantino, *Nucl. Phys.* **B633**, 212 (2002); C. Tarantino, *Eur. Phys. J. C* **33**, s895 (2003); A. J. Lenz, *AIP Conf. Proc.* **1026**, 36 (2008).

- [2] K. Nakamura *et al.* (Particle Data Group), *J. Phys. G* **37**, 075021 (2010).

- [3] I. Bigi *et al.*, in *B Decays*, edited by S. Stone (World Scientific, Singapore, 1994), 2nd ed.

- [4] F. Gabbiani, A. Onischenko, and A. Petrov, *Phys. Rev. D* **68**, 114006 (2003); **70**, 094031 (2004).
- [5] N. G. Uraltsev, *Phys. Lett. B* **376**, 303 (1996); D. Pirjol and N. G. Uraltsev, *Phys. Rev. D* **59**, 034012 (1999); P. Colangelo and F. De Fazio, *Phys. Lett. B* **387**, 371 (1996); M. Di Pierro, C. T. Sachrajda, and C. Michael, *Phys. Lett. B* **468**, 143 (1999).
- [6] A. Abulencia *et al.* (CDF Collaboration), *Phys. Rev. Lett.* **98**, 122001 (2007).
- [7] T. Aaltonen *et al.* (CDF Collaboration), *Phys. Rev. Lett.* **104**, 102002 (2010).
- [8] A. Sill *et al.*, *Nucl. Instrum. Methods Phys. Res., Sect. A* **447**, 1 (2000).
- [9] T. Affolder *et al.*, *Nucl. Instrum. Methods Phys. Res., Sect. A* **526**, 249 (2004).
- [10] CDF II uses a cylindrical coordinate system in which ϕ is the azimuthal angle, r is the radius from the nominal beam line, and z points in the proton beam direction with the origin at the center of the detector. The transverse plane is the plane perpendicular to the z axis. The \hat{x} axis points outward from the accelerator ring, and the \hat{y} axis points upwards.
- [11] G. Ascoli *et al.*, *Nucl. Instrum. Methods Phys. Res., Sect. A* **268**, 33 (1988).
- [12] T. Dorigo *et al.*, *Nucl. Instrum. Methods Phys. Res., Sect. A* **461**, 560 (2001).
- [13] E. J. Thomson *et al.*, *IEEE Trans. Nucl. Sci.* **49**, 1063 (2002).
- [14] G. Punzi, [arXiv:physics/0401045v1](https://arxiv.org/abs/physics/0401045v1).
- [15] K. Abe *et al.* (Belle Collaboration), *Phys. Rev. D* **71**, 072003 (2005); **71**, 079903(E) (2005).